Spin fluctuations in $Sr_{1.6}Ba_{0.4}RuO_4$: An inelastic neutron scattering study with polarization analysis

Z. W. Li,[1,*] H. Guo,[1] C.-F. Liu,[1] F. Bourdarot,[2] W. Schmidt,[3] M. Skoulatos,[4] and A. C. Komarek[1,†]

[1]*Max-Planck-Institute for Chemical Physics of Solids, Nöthnitzer str. 40, D-01187 Dresden, Germany*

[2]*Institut Laue-Langewin (ILL), 71 avenue des Martyrs, F-38042 Grenoble Cedex 9, France*

[3]*Jülich Centre for Neutron Science JCNS, Forschungszentrum Jülich GmbH, Outstation at ILL, 71 avenue des Martyrs, F-38042 Grenoble Cedex 9, France*

[4]*Laboratory for Neutron Scattering, Paul Scherrer Institute, CH-5232 Villigen, Switzerland*

(Received 12 October 2016; revised manuscript received 19 December 2016; published 4 January 2017)

We present inelastic neutron scattering measurements on the ruthenate $Sr_{1.6}Ba_{0.4}RuO_4$ which is on the hitherto almost unknown Ba-substituted side of the doping phase diagram of $Sr_{2-x}Ae_xRuO_4$ (Ae = Ca, Ba). Unlike the Ca-substituted side of the phase diagram no (quasi)static magnetic peaks can be observed in $Sr_{1.6}Ba_{0.4}RuO_4$. Instead, incommensurate spin fluctuations can be observed around $\mathbf{q}_0 = (\pm 0.3, \pm 0.3, 0)$. Both the absolute intensity of $\chi''(\mathbf{Q},\omega)$ and its energy and temperature dependence as well as the anisotropy ratio $\chi''_c/\chi''_{a,b}$ resemble the ones in Sr_2RuO_4. Hence, a random potential implied by the substitution of huge Ba ions as well as the induced increase of interatomic distances has less impact on the magnetic properties than octahedral tilts implied by Ca substitution. Moreover, any ferromagnetic spin fluctuations are either absent in $Sr_{1.6}Ba_{0.4}RuO_4$ or below the detection limit.

DOI: 10.1103/PhysRevB.95.045105

I. INTRODUCTION

Single-layered perovskite ruthenate oxides have attracted considerable interest basically arising from the observation of unconventional superconductivity in Sr_2RuO_4 [1–8]. Similar as in cuprates and iron based superconductors, it was found that the superconductivity in Sr_2RuO_4 also appears in close proximity to magnetic instabilities [1–4]. However, unlike the pairing symmetries found in the former two systems, superconductivity in Sr_2RuO_4 is believed to exhibit spin-triplet p-wave pairing [5–8]. It was naturally suggested that ferromagnetic (FM) spin fluctuations should be responsible for the pairing mechanism in Sr_2RuO_4[9]. Only weak FM spin fluctuations are indicated by neutron scattering measurements [10–13] and nuclear magnetic resonance (NMR) [5,14]. These coexist with stronger incommensurate antiferromagnetic (AFM) correlations [3,10,12] which appear at $\mathbf{Q}_0 = \mathbf{q}_0 + \mathbf{G}$ where $\mathbf{q}_0 = (\pm 0.3, \pm 0.3, 0)$. Alternatively, it was shown by theory that anisotropic antiferromagnetic spin fluctuations with $\chi''_c > \chi''_{a,b}$ can also give rise to the observed p-wave superconductivity [7,15]. Although slightly weaker than predicted by theory, an anisotropy of $\chi''_c/\chi''_{a,b} = 2 \sim 3$ has, indeed, been observed by NMR measurements [16] as well as by unpolarized and polarized neutron scattering measurements [10,17].

Chemical substitution turned out to yield interesting changes in Sr_2RuO_4[1,4,11,13,18]. Already at rather low concentration levels of ∼3% short ranged AFM ordering can be stabilized by the substitution of Ru by Ti/Mn [18,19]. Neutron studies attribute these AFM correlations to the same Fermi surface nesting effect between the α/β sheets that is also responsible for the incommensurate spin fluctuations in pure Sr_2RuO_4 [18]. On the other hand, short ranged FM order can be induced by the substitution of Ru by Co with a concentration level as low as ∼2% [19]. These results indicate vicinity of this system to AFM/FM correlations.

Further interest has been generated from the investigation of substitution of other elements into the SrO layers which leaves the Ru-O layer intact [1,4,11,13,20,21]. The $Sr_{2-x}Ca_xRuO_4$ system exhibits a rich phase diagram [1,4,11,22]. Extensive neutron scattering, muon spin rotation (μSR), and NMR measurements have been performed to study this system. The pure Ca_2RuO_4 compound is a Mott insulator that orders antiferromagnetically below 110 K [4]. Additional incommensurate AFM correlations along the vertical direction ([1/0 0/1 0] direction) was found to coexist with the diagonal ones [([1 ±1 0]) direction] in a broad composition range of the metallic phase [13,20]. Recently, a comprehensive magnetic phase diagram has been drawn which shows that magnetic order persists over nearly the entire substitution range of the $Sr_{2-x}Ca_xRuO_4$ system [1]. However, compared to the very well studied Ca-substituted side, much less is known about the Ba-substituted side. Whereas the unit cell volume continuously decreases with increasing Ca substitution which is accompanied by additional octahedral tilts [22], the unit cell volume continuously increases with increasing Ba substitution but without the change of the crystal structure [23]. Since it has been recently shown that the superconducting transition temperature of Sr_2RuO_4 can be strongly enhanced by strain [24–26], we decided to study the impact of Ba substitution in Sr_2RuO_4 [23]. Here, we report polarized neutron scattering experiments of $Sr_{1.6}Ba_{0.4}RuO_4$. Our measurements reveal the persistence of incommensurate magnetic fluctuations similar as in Sr_2RuO_4 and the absence of any (quasi)static spin correlations as observed for Ca substitution in $Sr_{1.5}Ca_{0.5}RuO_4$ [20].

II. EXPERIMENTAL

Single crystals of $Sr_{1.6}Ba_{0.4}RuO_4$ up to ∼100 mm in length and ∼6 mm in diameter were grown by the traveling solvent floating zone method [23]. The as-grown crystals have

*Current address: Institute of Applied Magnetics, Key Lab for Magnetism and Magnetic Materials of the Ministry of Education, Lanzhou University, Lanzhou 730000, China; zweili@lzu.edu.cn

†Komarek@cpfs.mpg.de

been characterized by powder x-ray diffraction, resistivity, and magnetization measurements. At room temperature, the lattice parameters of our studied $Sr_{1.6}Ba_{0.4}RuO_4$ single crystals amount to $a = 3.8926(3)$ Å and $c = 12.884(1)$ Å (space group $I4/mmm$). Since the neutron scattering intensity is usually extremely weak for ruthenates, we have co-aligned 14 single crystals of ∼50 g with a total mosaic spread of distinctly less than 1° [23] as has been characterized at the cold neutron triple-axis spectrometer RITA-II at the Paul Scherrer Institute, Villigen, Switzerland (with [100]/[010] orientation in the scattering plane).

Inelastic scattering experiments with polarized neutron were performed on this 50 g ensemble at the thermal triple-axis spectrometer IN22 at the ILL, Grenoble, France. Polarization analysis was obtained with a setup of Heusler (111) monochromator and analyzer both working in the vertical focusing and horizontal flat mode. In the entire paper we will use the suffix $x/y/z$ to denote the neutron polarization: (i) the x direction is parallel to the scattering vector $\mathbf{Q}$, (ii) the y direction is perpendicular to $\mathbf{Q}$ and within the scattering plane, and (iii) the z direction is perpendicular to the scattering plane. Spin-flip and non-spin-flip channels are denoted by SF and NSF, respectively. In order to suppress higher order neutron contamination a pyrolytic graphite filter was installed between sample and analyzer. The experiments were done with a fixed final neutron energy of 14.7 meV ($k_f = 2.662\,\text{Å}^{-1}$). The flipping ratio measured on (110) nuclear Bragg peak reflection amounts to $R \sim 16$.

III. RESULTS AND DISCUSSION

In Fig. 1(a) (H,1-H,0) scans at 4 meV are shown for the SFx and NSFx channels. Two magnetic peaks centered at $\mathbf{Q}_0 = (0.3,0.7,0)$ and $(0.7,0.3,0)$ can be seen in the SFx channel. These magnetic peak positions point to a propagation wave vector $\mathbf{q}_0 = (\pm 0.3,\pm 0.3,0)$, which is similar to that found in Sr_2RuO_4 [3,12,27] and Ti/Ca substituted compounds [11,13,18,20]. In addition to these peaks found in the diagonal scan direction, further peaks were also observed along vertical directions [(H00)/(0K0)] in $Sr_{2-x}Ca_xRuO_4$ [13]. However, in $Sr_{1.6}Ba_{0.4}RuO_4$ no similar observation can be made in scans through $\mathbf{Q} = (1,0,0)$ (i.e., in the vertical direction), see Fig. 1(b). Moreover, the absence of any magnetic signal at the two-dimensional ferromagnetic zone center (1 0 0) indicates that no spin fluctuations with FM character can be observed with polarized neutrons in $Sr_{1.6}Ba_{0.4}RuO_4$. In contrast to $Sr_{2-x}Ca_xRuO_4$ [13,20] also no (quasi)static AFM correlations can be found in $Sr_{1.6}Ba_{0.4}RuO_4$, see Fig. 1(a). The inset of Fig. 1(b) shows the low temperature magnetic susceptibility data (measured in a field of $H = 50$ Oe) which indicates the absence of superconductivity down to 0.5 K for this $Sr_{1.6}Ba_{0.4}RuO_4$ sample.

The imaginary part of the dynamical spin susceptibility $\chi''(\mathbf{Q},\omega)$ can be obtained after a correction for the detailed balance factor [28] by the equation

$$\frac{d^2\sigma}{d\Omega dE} = N\frac{k_f}{k_i}\frac{r_0^2}{4\pi\mu_B^2}|f(\mathbf{Q})|^2 e^{-2W} \times \sum_{\alpha,\beta}(\delta_{\alpha,\beta} - \hat{Q}_\beta\hat{Q}_\beta)\frac{\chi''_{\alpha,\beta}(\mathbf{Q},\omega)}{\left(1 - e^{-\frac{\hbar\omega}{k_BT}}\right)}, \quad (1)$$

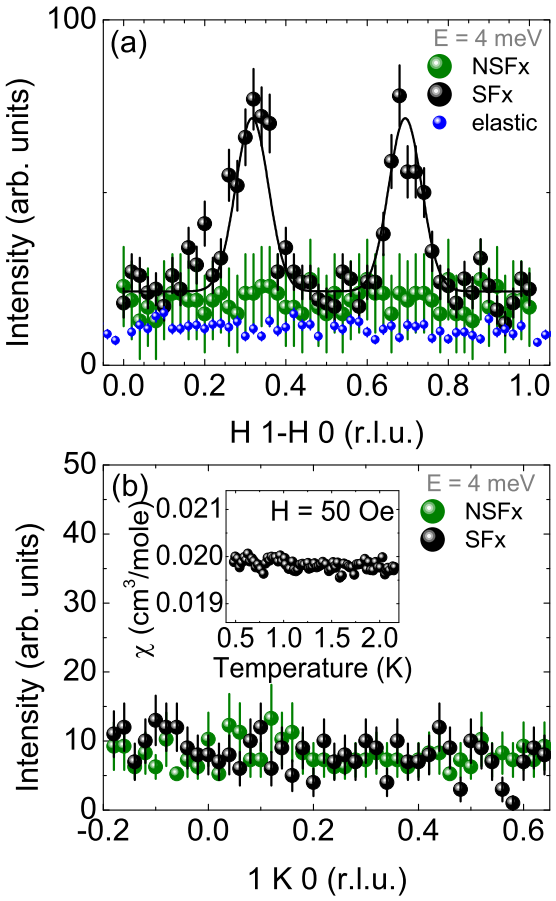

FIG. 1. (a) Constant energy (H,1-H,0) scans across the incommensurate magnetic peak positions with $E = 4$ meV and $T = 1.5$ K in both spin flip (SFx) and non-spin flip (NSFx) channels. Additionally, also the elastic scattering measured with unpolarized neutrons is shown (blue data points). (b) (1,K,0) scans measured with $E = 4$ meV and $T = 1.5$ K in both SFx and NSFx channels scanning across the two-dimensional zone center at (1,0,0) where ferromagnetic fluctuations should be observable. Inset of (b) shows the low temperature magnetic susceptibility data measured with $H = 50$ Oe indicating the absence of superconductivity down to 0.5 K. Solid line through the data points is best fit to a symmetric double Gaussian profile. Note, the NSFx data have been shifted vertically to the same background level of the SFx data for a better view.

where $f(\mathbf{Q})$ is the magnetic form factor of the Ru^+ ion as a good proximation [3]. For $\mathbf{Q}$ points within the ab plane the measured intensities in the spin flip channel can be simplified as [29]

$$\begin{aligned} I_x^{SF} &\propto \chi''_{a,b}(\mathbf{Q},\omega) + \chi''_c(\mathbf{Q},\omega) + I_{BKG} \\ I_y^{SF} &\propto \chi''_c(\mathbf{Q},\omega) + I_{BKG} \\ I_z^{SF} &\propto \chi''_{a,b}(\mathbf{Q},\omega) + I_{BKG}, \end{aligned} \quad (2)$$

where I_{BKG} is the background contribution in the spin flip channel. (Here, we have neglected nuclear contributions.)

Figure 2(a) shows scans across the incommensurate position at $\mathbf{Q}_0 = (0.7,0.3,0)$ that were measured in the SFx channel for several energy transfers up to $E = 20$ meV. We have

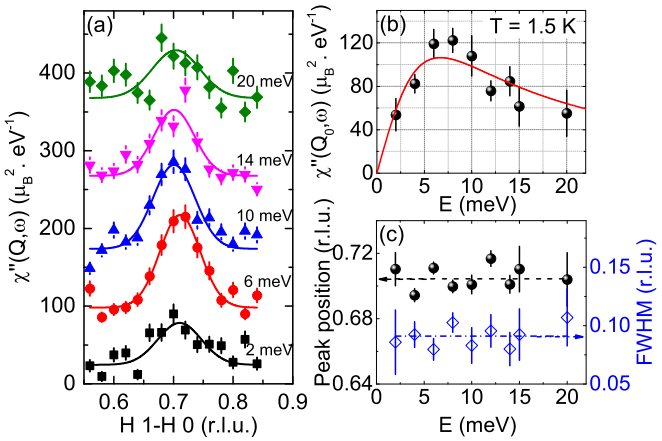

FIG. 2. (a) (H,1-H,0) scans across the incommensurate point $\mathbf{Q}_0 = (0.7,0.3,0)$ at 1.5 K in SFx channel with indicated transfer energies. Solid lines are Gaussian fits to the data. (b) Energy dependence of the imaginary part of the dynamical magnetic susceptibility at $\mathbf{Q}_0$ determined from the Gaussian fits. Red solid line is a fit to a single-relaxor function (see text). (c) The magnetic peak position and full width at half maximum (FWHM) as obtained from the fits are plotted as a function of transfer energy. Dash/dash-dotted arrows are guides to the eye.

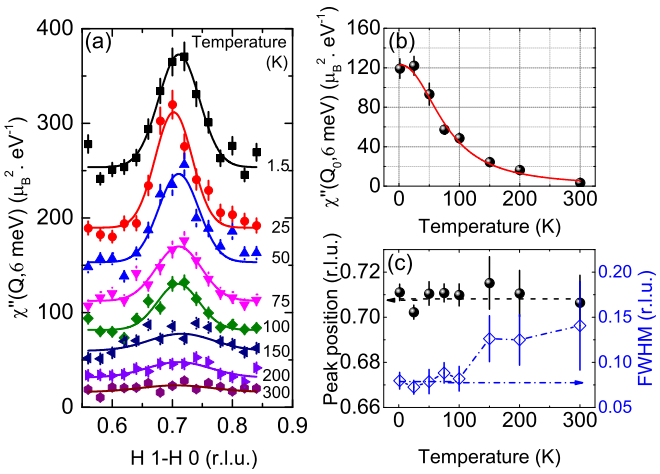

FIG. 3. (a) (H,1-H,0) scans across the incommensurate point $\mathbf{Q}_0 = (0.7,0.3,0)$ at indicated temperatures in SFx channel with an energy transfer of $E = 6$ meV. Solid lines are Gaussian fits to the data. (b) Temperature dependence of the imaginary part of the dynamical magnetic susceptibility at $\mathbf{Q}_0$ determined from the Gaussian fits. Red solid line is a guide to the eye. (c) The magnetic peak position and FWHM as obtained from the fits are plotted as a function of temperature. Dash/dash-dotted arrows are guides to the eye.

calibrated $\chi''(\mathbf{Q},\omega) = 2\chi''_{a,b} + \chi''_c$ in absolute units against acoustic phonons close to $\mathbf{Q} = (2,0,0)$ following a standard procedure [3,30]. The energy dependence of $\chi''(\mathbf{Q}_0,\omega)$ shown in Fig. 2(b) has been determined by Gaussian fits to the calibrated data shown in Fig. 2(a). $\chi''(\mathbf{Q},\omega)$ can be parameterized according to linear response theory (single-relaxor behavior) [3,29] by

$$\chi''(\mathbf{Q}_0,\omega) = \chi'(\mathbf{Q}_0,0)\frac{\Gamma\omega}{\omega^2+\Gamma^2}, \tag{3}$$

where Γ is the characteristic energy of 6.7(8) meV and $\chi'(\mathbf{Q}_0,0) = 209(11)\mu_B^2\, eV^{-1}$ corresponds to the static spin susceptibility at $\mathbf{Q}_0$. These values are comparable to that found in pure Sr_2RuO_4 with $\Gamma = 9$ meV and $\chi'(\mathbf{Q}_0,0) = 180\ \mu_B^2\ \mathrm{eV}^{-1}$ [3]. Note, one would expect two characteristic energies and amplitudes corresponding to $\chi''_{a,b}(\mathbf{Q},\omega)$ and $\chi''_c(\mathbf{Q},\omega)$ to fit the data in Fig. 2(b). However, such an analysis cannot be made for the current study which would require better statistics.

Peak positions and peak widths are shown as a function of energy transfer in Fig. 2(c). Averaging the peak width (FWHM) yields $\Delta\mathbf{Q} = 0.091(4)$ r.l.u. which corresponds to a correlation length of 9.4(4) Å that is almost identical to the values observed in Sr_2RuO_4. The spin fluctuations found in the highest Ba substituted sample $Sr_{1.6}Ba_{0.4}RuO_4$ are very similar to the ones observed in Sr_2RuO_4 [3]. Also the uniform susceptibility of $Sr_{1.6}Ba_{0.4}RuO_4$ exhibits a similar magnitude like that of Sr_2RuO_4 on the level of $\tilde{\chi} = \chi'(0,0) \sim 10^{-3}$ emu/mole being different from that on the Ca substituted side of the phase diagram [4,23].

The temperature dependence of the spin fluctuations in $Sr_{1.6}Ba_{0.4}RuO_4$ is shown in Fig. 3. With increasing temperature $\chi''(\mathbf{Q}_0,6)$ exhibits a sharp decrease with an extended tail that persists up to 300 K, see Fig. 3(b). A very similar temperature dependence has been observed in the parent compound

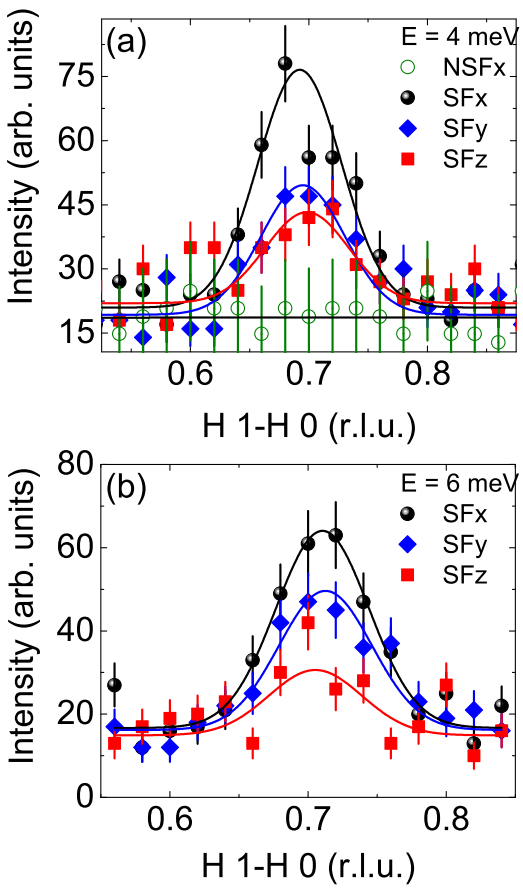

FIG. 4. Diagonal scans in all three (x,y,z) polarization channels across the incommensurate point $\mathbf{Q}_0 = (0.7,0.3,0)$ at $T = 1.5$ K with energy transfers of 4 meV and 6 meV are shown in panel (a) and (b), respectively. Solid lines through the data points are Gaussian fits.

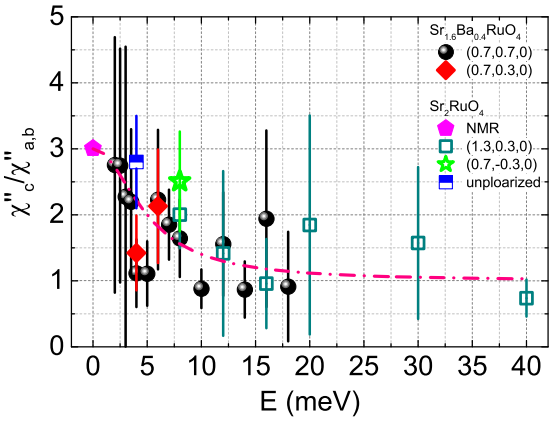

FIG. 5. Energy dependence of the anisotropy ratio $\chi_c''/\chi_{a,b}''$ of the incommensurate fluctuations measured at points $\mathbf{Q}_0 = (0.7,0.7,0)$ (black sphere) and $\mathbf{Q}_0 = (0.7,0.3,0)$ (red diamond) for $Sr_{1.6}Ba_{0.4}RuO_4$. The NMR result (pink pentagon) measured for Sr_2RuO_4 was taken from Ref. [16], and the polarized neutron data for Sr_2RuO_4 measured at points $\mathbf{Q}_0 = (1.3,0.3,0)$ (open square) and $\mathbf{Q}_0 = (0.7,-0.3,0)$ (open star) were taken from Ref. [10]. The unpolarized neutron data (half filled square) at 4 meV is from Ref. [17]. Dash dotted line is a guide to the eye.

Sr_2RuO_4 by neutron and NMR measurements [3,14]. The temperature dependence of peak positions and peak widths are shown in Fig. 3(c). Whereas no temperature dependence of the peak positions can be observed, a peak broadening can be observed with increasing temperature. These results can be understood within the Fermi surface nesting scenario. With increasing temperature, thermal hopping of electrons into unoccupied states smears out the Fermi surface, yielding a decrease of the dynamical spin susceptibility $\chi''(\mathbf{Q},\omega)$ and a broadening in $\mathbf{Q}$ space [3].

A detailed polarization analysis is shown in Fig. 4. Diagonal scans across $\mathbf{Q}_0 = (0.7,0.3,0)$ are shown for (a) 4 meV and (b) 6 meV energy transfer in the three different spin flip channels. According to equation (2) the anisotropy factor $\chi_c''/\chi_{a,b}''$ amounts to 1.2(6) and 2.2(9) for 4 meV and 6 meV, respectively. (We have assumed equal peak width for all three SF channels in the Gaussian fits and the integrated intensity have been used to calculate the anisotropy ratio. Note that the smaller anisotropy factor at 4 meV deviates from the trend (see Fig. 5) which we attribute to the insufficient statistics of the data due to the extremely weak signal in the ruthenate system.) These values are smaller than the NMR results for Sr_2RuO_4 where an anisotropy factor of 3 has been obtained [16]. However, our results yield similar values compared to neutron scattering measurements on Sr_2RuO_4 [10,17]. As observed for Sr_2RuO_4[10] the anisotropy of the incommensurate spin fluctuations in Sr_2RuO_4 decreases with increasing energy (and eventually becomes isotropic) which might also explain the bigger values observed in NMR experiments. We also made additional measurements at different $\mathbf{Q}$ points [i.e., $\mathbf{Q}_0 = (0.7,0.7,0)$]. The energy dependence of the anisotropy ratio $\chi_c''/\chi_{a,b}''$ determined from all these measurements is summarized in Fig. 5. The NMR results and neutron results for Sr_2RuO_4 [10,16,17] are also shown for comparison.

IV. SUMMARY

In conclusion, $Sr_{2-x}Ba_xRuO_4$ is a reference system for Sr_2RuO_4 that allows us to study the physical properties of this interesting system without altering its structural symmetries. Whereas the maximum Ca-substitution level amounts to $x_{\max}^{\mathrm{Ca}} = 2$ for $Sr_{2-x}A_xRuO_4$, due to a miscibility gap above $x_{\max}^{\mathrm{Ba}}$ on the other side of the phase diagram about ~40% is the corresponding maximum Ba-substitution level $x_{\max}^{\mathrm{Ba}}$ [23]. We found that the incommensurate spin fluctuations observed in Sr_2RuO_4 at $\mathbf{q}_0 \sim (\pm 0.3,\pm 0.3,0)$ still persist in $Sr_{1.6}Ba_{0.4}RuO_4$ at its maximum Ba-substitution level $x_{\max}^{\mathrm{Ba}}$ and that no (quasi)static spin correlations can be observed in the Ba-substituted side of the phase diagram $Sr_{2-x}Ba_xRuO_4$. This is unlike observations in the Ca-substituted side $Sr_{2-x}Ca_xRuO_4$ of the phase diagram. Thus, the random potential implied by Ba substitution and the increase of interatomic distances seems to have a different effect than changes due to local octahedral tilts arising from Ca substitution. The incommensurate spin fluctuations in $Sr_{1.6}Ba_{0.4}RuO_4$ resemble the ones observed in Sr_2RuO_4 including their absolute values of magnitude, the anisotropy factor, and their energy and temperature dependencies. Moreover, within our measurement accuracy FM spin fluctuations were found to be absent in nonsuperconducting $Sr_{1.6}Ba_{0.4}RuO_4$ (50 g of co-aligned single crystals).

ACKNOWLEDGMENTS

We thank L. H. Tjeng for helpful discussions. Moreover, we thank the team of H. Borrmann for powder x-ray diffraction measurements, the team of G. Auffermann for ICP measurements, and C. Klausnitzer for SQUID measurements.

[1] J. P. Carlo, T. Goko, I. M. Gat-Malureanu, P. L. Russo, A. T. Savici, A. A. Aczel, G. J. MacDougall, J. A. Rodriguez, T. J. Williams, G. M. Luke, C. R. Wiebe, Y. Yoshida, S. Nakatsuji, Y. Maeno, T. Taniguchi, and Y. J. Uemura, Nat. Mater. **11**, 323 (2012).

[2] A. P. Mackenzie and Y. Maeno, Rev. Mod. Phys. **75**, 657 (2003).

[3] Y. Sidis, M. Braden, P. Bourges, B. Hennion, S. NishiZaki, Y. Maeno, and Y. Mori, Phys. Rev. Lett. **83**, 3320 (1999).

[4] S. Nakatsuji and Y. Maeno, Phys. Rev. Lett. **84**, 2666 (2000).

[5] K. Ishida, H. Mukuda, Y. Kitaoka, K. Asayama, Z. Q. Mao, Y. Mori, and Y. Maeno, Nature (London) **396**, 658 (1998).

[6] G. M. Luke, Y. Fudamoto, K. M. Kojima, M. I. Larkin, J. Merrin, B. Nachumi, Y. J. Uemura, Y. Maeno, Z. Q. Mao, Y. Mori, H. Nakamura, and M. Sigrist, Nature (London) **394**, 558 (1998).

[7] T. Kuwabara and M. Ogata, Phys. Rev. Lett. **85**, 4586 (2000).

[8] K. Ishida, H. Mukuda, Y. Kitaoka, Z. Q. Mao, H. Fukazawa, and Y. Maeno, Phys. Rev. B **63**, 060507 (2001).

[9] I. I. Mazin and D. J. Singh, Phys. Rev. Lett. **79**, 733 (1997).
[10] M. Braden, P. Steffens, Y. Sidis, J. Kulda, P. Bourges, S. Hayden, N. Kikugawa, and Y. Maeno, Phys. Rev. Lett. **92**, 097402 (2004).
[11] O. Friedt, P. Steffens, M. Braden, Y. Sidis, S. Nakatsuji, and Y. Maeno, Phys. Rev. Lett. **93**, 147404 (2004).
[12] M. Braden, Y. Sidis, P. Bourges, P. Pfeuty, J. Kulda, Z. Mao, and Y. Maeno, Phys. Rev. B **66**, 064522 (2002).
[13] P. Steffens, O. Friedt, Y. Sidis, P. Link, J. Kulda, K. Schmalzl, S. Nakatsuji, and M. Braden, Phys. Rev. B **83**, 054429 (2011).
[14] T. Imai, A. W. Hunt, K. R. Thurber, and F. C. Chou, Phys. Rev. Lett. **81**, 3006 (1998).
[15] M. Sato and M. Kohmoto, J. Phys. Soc. Jpn. **69**, 3505 (2000).
[16] K. Ishida, H. Mukuda, Y. Minami, Y. Kitaoka, Z. Q. Mao, H. Fukazawa, and Y. Maeno, Phys. Rev. B **64**, 100501 (2001).
[17] T. Nagata, M. Urata, H. Kawano-Furukawa, H. Yoshizawa, H. Kadowaki, and P. Dai, Phys. Rev. B **69**, 174501 (2004).
[18] K. Iida, J. Lee, M. B. Stone, M. Kofu, Y. Yoshida, and S. Lee, J. Phys. Soc. Jpn. **81**, 124710 (2012).
[19] J. E. Ortmann, J. Y. Liu, J. Hu, M. Zhu, J. Peng, M. Matsuda, X. Ke, and Z. Q. Mao, Sci. Rep. **3**, 2950 (2013).
[20] S. Kunkemöller, A. A. Nugroho, Y. Sidis, and M. Braden, Phys. Rev. B **89**, 045119 (2014).
[21] P. Steffens, Y. Sidis, P. Link, K. Schmalzl, S. Nakatsuji, Y. Maeno, and M. Braden, Phys. Rev. Lett. **99**, 217402 (2007).
[22] O. Friedt, M. Braden, G. André, P. Adelmann, S. Nakatsuji, and Y. Maeno, Phys. Rev. B **63**, 174432 (2001).
[23] Z. Li, C.-F. Liu, M. Skoulatos, L. Tjeng, and A. Komarek, J. Cryst. Growth **427**, 94 (2015).
[24] Y. A. Ying, N. E. Staley, Y. Xin, K. Sun, X. Cai, D. Fobes, T. J. Liu, Z. Q. Mao, and Y. Liu, Nat. Commun. **4**, 2596 (2013).
[25] S. Kittaka, H. Taniguchi, S. Yonezawa, H. Yaguchi, and Y. Maeno, Phys. Rev. B **81**, 180510 (2010).
[26] C. W. Hicks, D. O. Brodsky, E. A. Yelland, A. S. Gibbs, J. A. N. Bruin, M. E. Barber, S. D. Edkins, K. Nishimura, S. Yonezawa, Y. Maeno, and A. P. Mackenzie, Science **344**, 283 (2014).
[27] K. Iida, M. Kofu, N. Katayama, J. Lee, R. Kajimoto, Y. Inamura, M. Nakamura, M. Arai, Y. Yoshida, M. Fujita, K. Yamada, and S.-H. Lee, Phys. Rev. B **84**, 060402 (2011).
[28] T. Chatterji, in *Neutron Scattering from Magnetic Materials*, edited by T. Chatterji (Elsevier Science, Amsterdam, 2006), pp. 1–24.
[29] L. Regnault, in *Neutron Scattering from Magnetic Materials*, edited by T. Chatterji (Elsevier Science, Amsterdam, 2006), pp. 363–395.
[30] G. Xu, Z. Xu, and J. M. Tranquada, Rev. Sci. Instrum. **84**, 083906 (2013).